ROTATION OF SHEAR-WAVE COMPONENTS AT NON-NORMAL ANGLES OF INCIDENCE: BLACK-BEAR DATA, OKLAHOMA

Terence A. Campbell

Department of Geological Sciences
The University of Texas at Austin

ABSTRACT

Analysis of seismic shear wave information is useful in characterizing properties of the media they travel through. Alford (1986) introduced a method of rotating combinations of observed seismic traces from orthogonal pairs of shear-source and shear-receiver components to identify the azimuthal orientations of symmetry axes of birefringence. This method has been widely applied to interpretation of subsurface fracture properties. As currently applied, this analysis is limited to zero-offset reflections, which results because the normal incidence reflection response is identical for SV and SH reflectivity. For non-normal incidence angles, however, there is a pronounced difference in SV and SH reflectivity as source-receiver offsets increase, leading to significant distortion in the polarity of the reflected shear wave. Polarization distortion due to the reflection process in typical 3D acquisition geometry is demonstrated and a correction to the polarization distortion is presented. The only information required for the correction is the angles of SV and SH zero crossings, typically at angles near 20° for SV and 40° for SH for most sedimentary rocks. This correction can be applied to the four horizontal components of 9C direct shear data at non-zero source-receiver offsets. The application of this 'corrected' analysis leads to an extension of the widely applied Alford rotation method to a wide range of reflection angles of incidence, and inclusion of a wide range of source-receiver offsets in pre-stack data. Examples of this analysis are given for both synthetic and field (Black Bear, Oklahoma) data.

INTRODUCTION

Internal properties of rocks such as anisotropy associated with cracks, fractures and the presence of clay minerals in shales is characterized by the analysis of variations in the transverse polarization of propagating seismic shear waves. The application of this technique is simplified by utilizing a single S-wave propagation path and analysis of variations in shear-wave polarization directions. S-waves may ultimately be polarized in the natural symmetry axes of anisotropic or transversely isotropic medium. In particular, a fast shear component (S1) propagating parallel to the fracture orientation, will be polarized in the direction of the higher

velocity of a transversely isotropic medium, whereas the slower shear component (S2) will be polarized orthogonal to S1. Thus, for transversely isotropic media, the S1 and S2 polarization directions may be proxies for geological parameters such as fracture or bedding orientation.

Alford (1986) introduced an analysis method of rotating combinations of observed seismic traces from orthogonal pairs of horizontal shear-source and shear-receiver components to identify the azimuthal orientations of symmetry axes of birefringence associated with a simplified anisotropy symmetry commonly defined as azimuthal anisotropy with a horizontal axis of symmetry (HTI). This method has been quite widely applied in interpretation of subsurface fracture properties by assuming fracturing it related to HTI anisotropy. Numerous published studies illustrate the efficacy of Alford rotation analysis for estimating anisotropy as a proxy for fracture characteristics. The limitation of the Alford's rotation is that it is valid only for normal incidence (1D) reflection. This results because the normal incidence reflection response is identical for SV and SH (relative to a common Cartesian coordinate system) reflectivity. For non-normal incidence angles, however, there is a pronounced difference in SV and SH reflectivity as source-receiver offsets increase, which leads to the significant distortion in the polarity of the reflected shear wave relative to the source polarization (Figure 1).

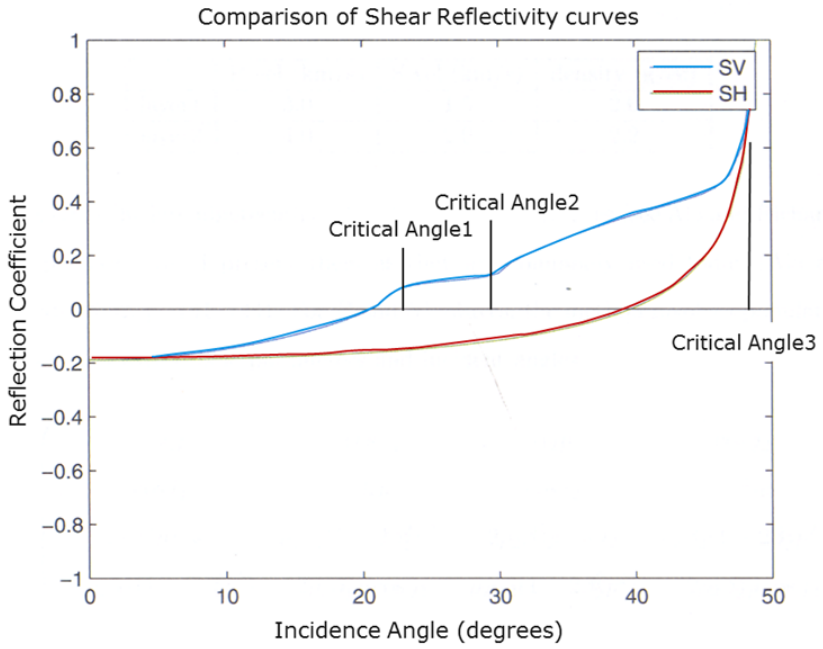

Figure 1. Reflection coefficients for SV-SV (blue) and SH-SH (red) waves showing that the reflection coefficients vanish at some particular angle of incidence. Velocity and density information for all the examples are given in table 1.The position of the three critical incidence angles are shown. The three critical angles relate to the P-wave mode-converted and refracted wave into the lower layer (22°), the internally refracted mode-converted P-wave in the upper medium (30°) and the refracted S-wave in the lower layer (49°). The zero crossing is at 20° for SV and 40° for SH.

Reflection of an arbitrarily polarized shear wave is described in terms of SH and SV components relative to the vertical plane connecting the source and receiver position (Figure 2). For acquisition of 3D seismic data with fixed orientations of horizontal sources and receivers in a planar distribution of source and receiver positions over Earth's surface, the vertical plane connecting individual source and receiver orientations does NOT, in general, align solely with the SV or SH orientations associated with vertical profile defined by the source and receiver locations. A simplified 3D acquisition design is shown in Figure 3, where the source polarization is in the east direction ($\Psi = 0$), a source-receiver azimuth at θ, and a pair of shear-receiver components oriented in the X-Y, or east and north, directions will record a shear-wave, reflected at the mid-point, with a polarization oriented an angle L; very different than the original source polarization. As seen in Figure 1, due to the difference in SV and SH reflection coefficients, there is a large polarization distortion occurring in the reflected shear-wave and we postulate we can remove this distortion by removing the AVO from the SV and SH components.

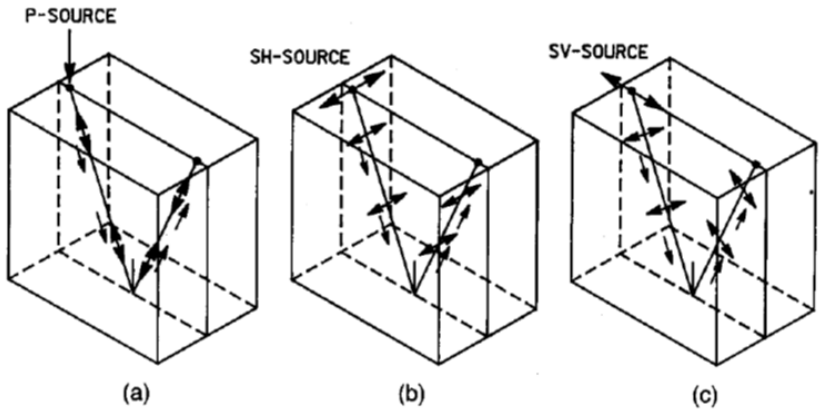

Figure 2. Ray propagation and polarization directions, with propagation shown by smaller arrows next to rays, and particle motion shown by two-headed arrows for (a) P-P, (b) SH-SH and (c) SV-SV waves (Tatham and McCormack, 1991). Note that P-wave particle motion is parallel to the propagation direction and in the vertical plane defined by the source and receiver position. SV particle motion is normal to the propagation direction and in the vertical plane. SH particle motion is normal to the propagation direction and normal to the vertical plane. The particle motion of the SH wave is always horizontal but the particle motion of SV wave although in the vertical plane, is not, in general, horizontal. In general, a propagating shear wave will have an arbitrary polarization normal (transverse) to the propagation direction. For most calculations, physics suggest that we address any shear-wave polarization in terms of orthogonal SV and SH components.

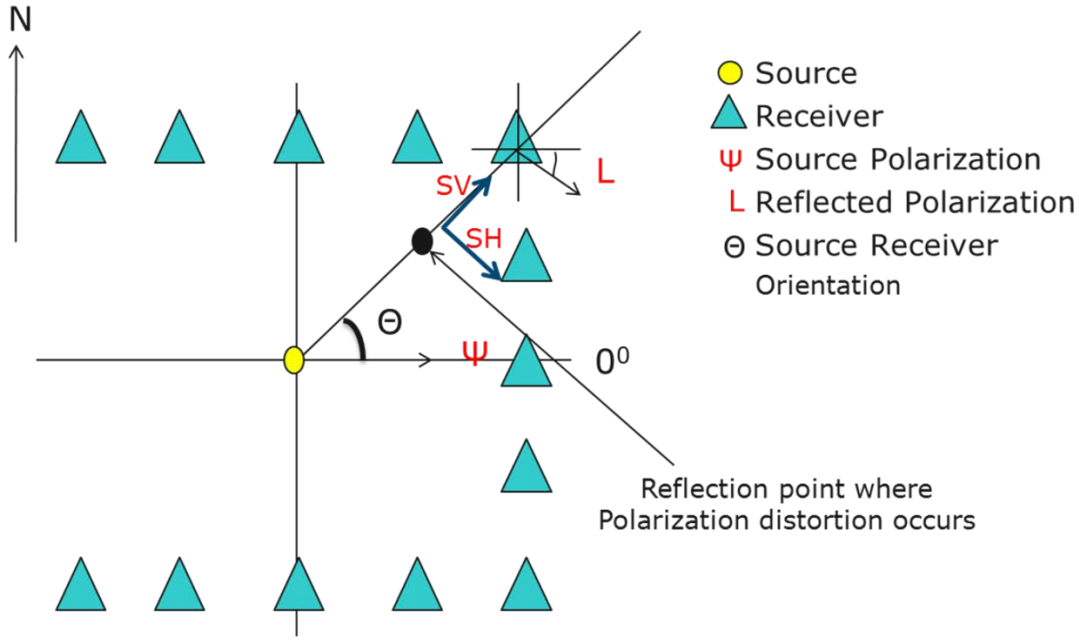

Figure 3. The acquisition geometry of a source position in a 3D direct shear survey with a source polarization of 0°, where L is the polarization of the reflected wave is calculated. Note the significant derivation of the reflected shear-wave from the original source polarization (modified from Lyons, 2006).

METHODOLOGY

Simmons (2001) indicated that the variations in azimuth and not the AVO is the reason for the polarization distortion observed. Campbell and Tatham (2011) demonstrated that corrections to this polarization distortion may be realized by correcting for the Amplitude Variations with Angles of incidence (or Offset) AVO, observed in the separate SV-SV and SH-SH reflections curves observed in Figure 1. The polarization of a single shear source can then be projected to SV and SH components for the vertical plane defined by the source and receiver positions, the corrections for the different amplitudes for the SV and SH components applied by normalization to zero offset, and then the polarization of the reflected shear wave determined by the orthogonal horizontal receiver components at the receiver position. To correct for this distortion we must demonstrate correction for SV and SH at each source-receiver azimuth.

Firstly, we apply simplifying assumptions for the Zoeppritz equation proposed by Spratt et al. (1993) and Lyons (2006). Spratt et al. (1993) proposed using typical assumptions of small incidence angles and small contrasts in velocities and density to give the following forms for the SV-SV and SH-SH reflectivity relations:

$$R_{sv\text{-}sv} = A + B_{sv} \sin^2\Theta \qquad (1)$$

and

$$R_{sh\text{-}sh} = A + B_{sh} \sin^2\Theta. \qquad (2)$$

Lyons (2006), based on some of the simplifying assumptions, modified the SH reflectivity to:

$$R_{sh\text{-}sh} = A + B_{sh} \tan^2\Theta. \qquad (3)$$

Because both the SV-SV and SH-SH reflectivity curves do have zero crossing at relatively modest angles of incidence for typical values of velocities and densities encountered in sedimentary rocks (near 20° for SV and 40° for SV), we can use these simplified $\sin^2$ and $\tan^2$ relations to estimate the actual Zoeppritz equations to select the values of the zero crossing angles. Since we are correcting to zero offset, A is set to unity. B is estimated from knowledge of A (unity) and the value of the amplitude (zero) at the zero crossing estimated from the simplified Zoeppritz' equations. Significantly, the only parameter required for the calculation of the correction is the value of the zero crossing. (Spratt et al. 1993, Gumble, 2006, Lyons, 2006).

A simulated example using of this polarization distortion and correction for a single shear source polarization in an isotropic medium is illustrated in Figure 4. The model parameters used for the isotropic medium is shown in Table 1. The uncorrected data (Figure 4) shows significant polarization distortion of the single source polarizations at offsets near the SV zero-crossing. The corrected data (Figure 5) show a quite consistent conformity to the observed reflection polarizations relative to source polarization at angles approaching the SH zero crossing. A singularity in the correction occurs at the SV zero crossing, and thus data are 'muted' near this offset.

Table 1. Two layer isotropic model with elastic and seismic properties.

Model Parameters	
Layer 1 (Isotropic layer)	Vp=3.0km/sec Vs=1.5km/sec ρ=2.00g/cm3 h=2.00 km
Layer 2 (Isotropic half space)	Vp(0)=4.0km/sec Vs(0)=2.0km/sec ρ=2.2g/cm^3

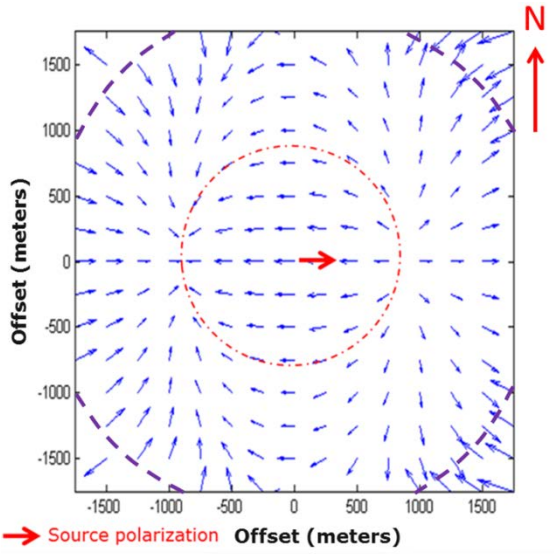

Figure 4. Computed polarizations of shear-wave reflections in a single 3D source record (source at center) of a 3D survey of isotropic media (map view) corresponding to a reflector depth of 2000m. Two horizontal components (east and north) of particle motion are observed at receiver locations spatially distributed on the surface. The length of the vectors indicate the amplitude of the reflected wave, and the orientation of the vectors indicates the observed polarization (source is polarized due east). Note the wide variation in polarization over the surface. The red circle shows the offset associated with the zero-crossing of the SV reflection. The purple dashed lines shows the offset associated with the zero-crossing of the SH reflection. Note the change in polarization at the SV zero crossing position as source-receiver offset increases. Note the strong polarization distortion at increased offset. At approximately 1250 meters the arrows switch polarity direction representing the SH-SH zero-crossing.

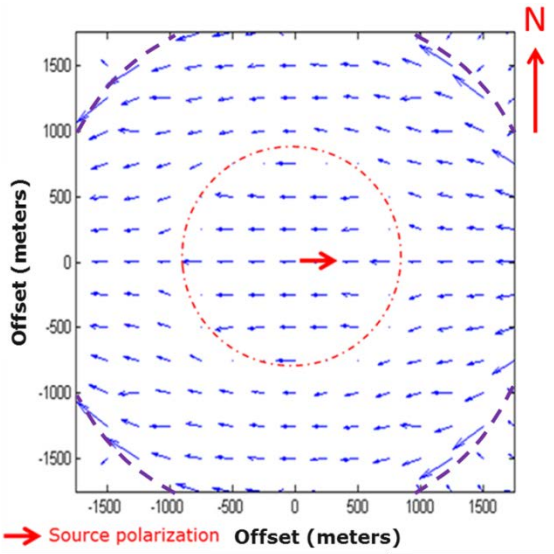

Figure 5. Polarization corrections applied to the simulated polarization distortions in a 3D record of isotropic media (map view) corresponding to a reflector depth of 2000m. The original polarization data is shown in Figure 4. The length of the vectors indicate the amplitude of the data, and the orientation of the vectors indicates the observed polarization (source is polarized due east). The corrections used a zero crossing of 22° SV and 40° for actual velocities used in the modeling. The purple dashed lines shows the offset associated with the zero-crossing of the SH reflection.

Extension of Alford's Rotation to non-Normal Incidence Angles

We propose to extend the Alford (1986) rotation to non-normal angles of incidence by minimizing the polarization distortion upon reflection for each source component for all the receiver locations associated with this source position. This will lead to four traces associated with a given pair of source and receiver positions in the survey. The HTI anisotropy, 'cross-term' energy is for the four-trace sets produced when wave source polarizations are at an arbitrary angle relative to the principal axes of symmetry of the HTI anisotropy. By applying Alford (1986) rotation analysis which is only valid for normal angles of incidence we can remove this cross term energy in the presence of no HTI anisotropy. Hence, we hypothesize that by applying the proposed polarization correction to the original multi-offset data prior to applying Alford's rotation should extend rotation analysis to include non-normal angles of incidence. This is illustrated with an example applied to synthesized data generated by a method of Mallick and Frazer (1987). The parameters for this single reflector between an isotropic and anisotropic layer are given in Table 2. The anisotropy of the lower layer does impose a polarity modification upon reflection (Campbell and Tatham, 2012), which is preserved during propagation through the isotropic upper layer to the surface.

Table 2. Properties of an isotropic media, VP is the P-wave velocity, VS is the shear wave velocity. VP(0) and VS(0) are the vertical P- and S- velocities in the HTI medium, and ε, δ, and γ are the Thomsen(1986) parameters.

Model Parameters	
Layer 1 (Isotropic Layer)	Vp=3.0km/sec Vs=1.5km/sec ρ=2.00g/cm^3 h=2.00 km
Layer 2 (Anisotropic Layer)	Vp = 4.0km/sec Vs = 3.0km/sec ε = 0.30 δ = 0.1 γ = 0.2 ρ=2.2g/cc

The simulated data for the isotropic over anisotropic model for a 2D shot record oriented at 30° to the fracture direction is shown in Figure 6. The fracture orientation is in the X direction of an X-Y survey grid, with both the source and receiver orientations in the X and Y directions. Note that offsets are represented by angles of incidence from 0 to 45 degrees. The four panels are for traces from the X-oriented source into the X oriented receivers (X-X) in the survey grid, Y-oriented source recorded by X oriented receivers (Y-X), X oriented source and Y oriented

receivers (X-Y) and Y oriented source and Y Zoeppritz equations, the zero crossings for the SV-SV and SH-SH reflectivity are near 20° and 40°, respectively. Since none of the four shot records is purely SH-SH or SV-SV, we fail to fully isolate the zero-crossings. Do note, however, that the energy is concentrated in the X-X and Y-Y quadrants. At angles of incidence beyond about 25°, there is energy in both the diagonal and off-diagonal quadrants.
oriented receivers (Y-Y). In the zero-offset analysis using current Alford rotation methods, the applicable data would be limited to only four traces, X-X, Y-X, X-Y and Y-Y for the zero offset values. From the

Figure 7 shows the same data with the appropriate polarization corrections applied to all offsets to compensate for the SV and SH effects. Then we apply the Alford's rotation to account for the fracture direction. Note the minimal energy in the off-diagonal Y-X and X-Y cross-terms, especially at larger angles of incidence. I expand the discussion of synthetic examples of polarized shear-wave reflections to real field direct shear-source data from the Black Bear 3D 9C seismic survey. The Black Bear survey is located in Northeast corner of Stephens county Oklahoma in the Ardmore Basin. Tectonically the Ardmore basin lies in the foreland of the Ouachita fold and thrust belt and within the splays of the Washita Valley wrench system. The surface seismic data were gathered in 1998 by The University of Texas at Austin's Bureau of Economic Geology (Exploration Geophysics Laboratory) and graciously provided for this study. Surface areal coverage is 42 km^2 (15 square miles). Discussions of the published results of shear-wave polarizations interpreted from a 9C VSP in the Brady well about 30 km from the surface survey are also included (Beckham, 1996). We demonstrate from the data set where a preliminary scan of rotations shows total energy in the X-X and Y-Y (diagonal) quadrants and the Y-X and X-Y off-diagonal quadrants is summarized in Figure 8. This result is simply the sum of all angles of incidence for the entire range of incidence angles in the shot record for each of the quadrant pairs Note the maximum energy occurs at the 30° rotation angle (and the minimum in energy for the off-diagonal terms), consistent with the expected polarization for the model.

Extending the Alford's rotation to non-normal angles of incidence was applied the Black Bear seismic data set, Oklahoma and due to the high levels of anisotropy >10% it was quite difficult to identify if the correction works or does not work. We know it works on simulated data as shown in Figures 6 and 7 but we do need to find a more robust data set to apply the correction too.

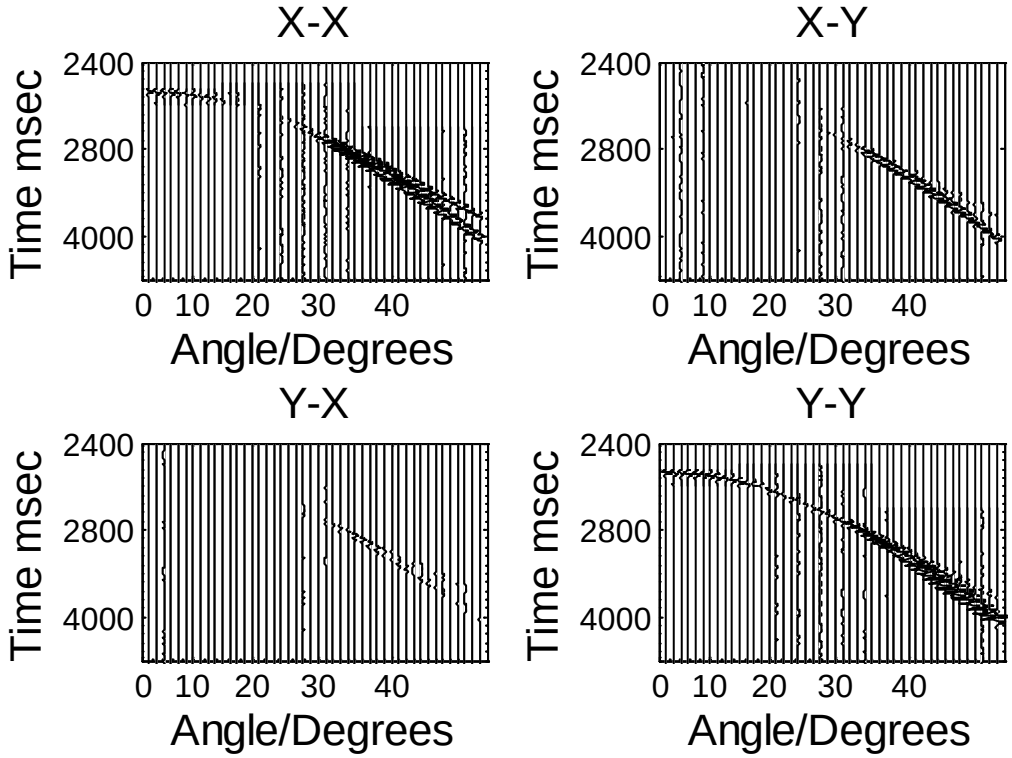

Figure 6. Synthetic data from the two layer models isotropic/ anisotropic model outlined in Table 2. The layer depth at 2km. Columns are X (east) and Y (north) sources, rows are X (east) and Y (north) receivers, in the original field coordinates. . Note zero crossing occurs at 22° for X-X and 40° for Y-Y panels with cross-term energy being present indicating anisotropy. The zero crossing on the Y-Y panel is difficult to see because of out of plane energy being present. Note the change in trace amplitude from 0° to 40°. No polarization of rotations has been applied.

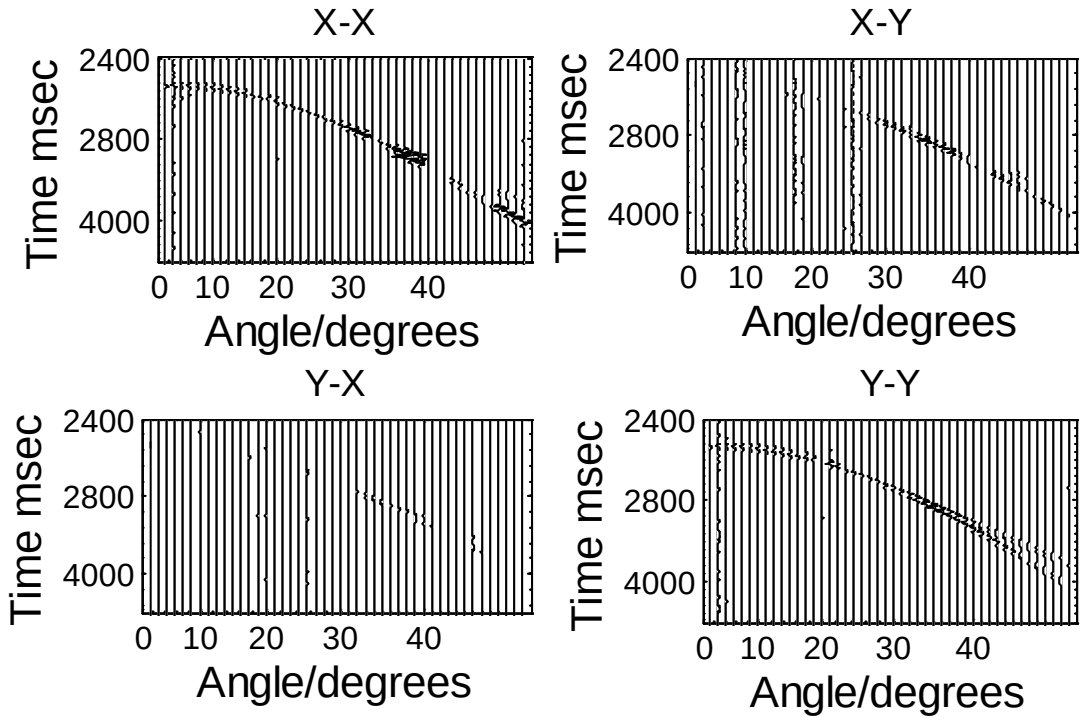

Figure 7. Synthetic data from the two layer model isotropic/ anisotropic model after polarization correction. The layer depth at 2km. Columns are X (east) and Y (north) sources, rows are X (east) and Y (north) receivers, in the original field coordinates. Note constant amplitude of X-X and Y-Y panels and how the cross-term energy changes after polarization correction has been applied. Also the zero crossing (40°) on the Y-Y synthetic seismic but other traces are also muted due to the high amplitude nature after polarization correction is applied.

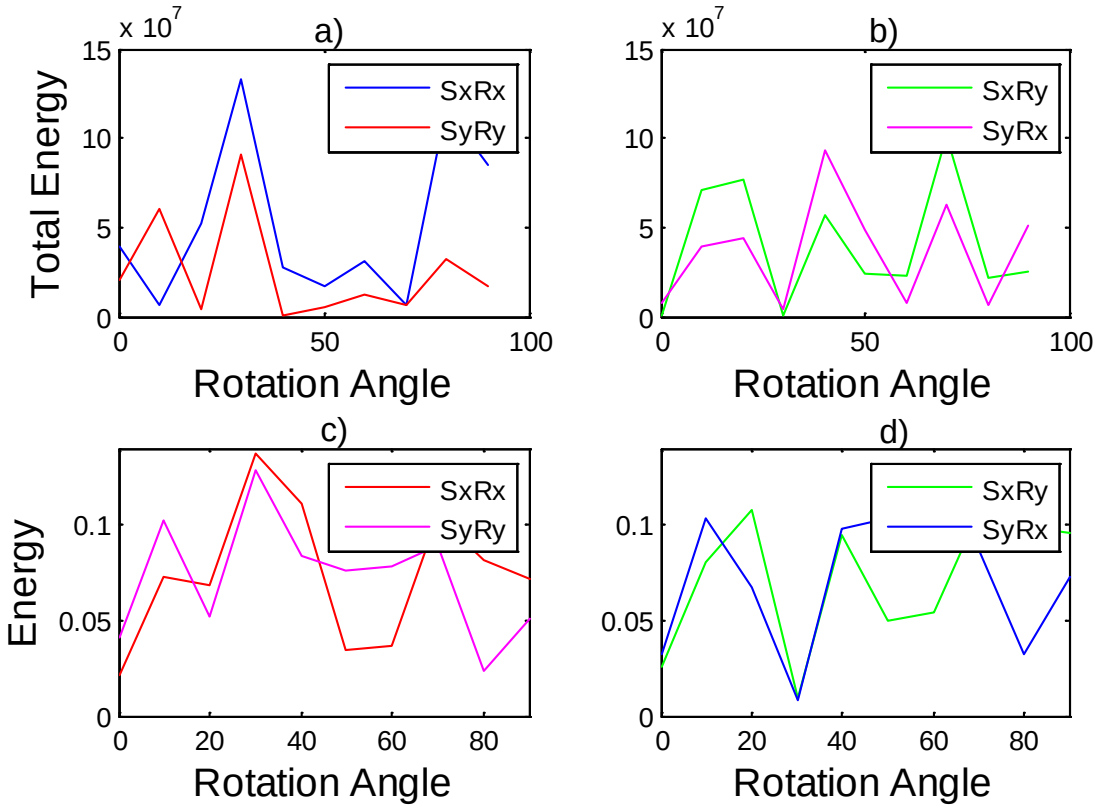

Figure 8. Results of the proposed Alford-like rotation polarization scan applied to horizontal components of 9C shear synthetic models (a) and (b)—for a range of incidence angles from 0-40°—and from polarization azimuths of 0° to 90°. The rotation process projects these polarizations to coordinates consistent with the HTI geometry, and is used to estimate where the cross-term energy is minimized. The numerical model has a 2 km thick isotropic layer over an HTI anisotropic layer with a 30° 'fracture' strike direction. The plot correctly indicates minima in cross-term energy at 30° and the X-X and Y-Y receiver pairs are maxima. At all other rotation angles, the cross-term energy is not zero, meaning it's not at the correct orientation. Results of a similar analysis applied to the four horizontal receiver components X (east) and Y (north) source and X (east) and Y (north) of the 9C Oklahoma Black Bear field data (c) and (d). A similar analysis was applied to a reflector at a shear-wave reflection time of 1.1 seconds. Similar to the synthetic data, there is energy on the cross-terms, which is indicative of anisotropy. Cross-term energy is a minimum at 30° and aligned X-X and Y-Y receiver pairs are energy maxima. Analysis of 9C VSP and crossed-dipole data in a nearby well (Texaco # 1 Brady Ranch) shows strong HTI anisotropy, at a 30° azimuth, in the entire shallow part of the section.

DISCUSSION AND CONCLUSIONS

Anisotropy presents a particular challenge and opportunity in understanding the ever expanding shale gas plays. On land seismic data, some have approached the acquisition problem by restricting the data to very small offsets and have attempted to deal with the overwhelming ground roll interference by the use of source and receiver arrays and/or abundant trace mixing in data processing. Others have rotated horizontal components into S1 and S2 directions extracted from nearby VSP studies. Still others have worked entirely in SV and SH components. We indicated that azimuthal anisotropy effects can then be recognized and analyzed by monitoring the reflection signal (in radial transverse coordinates) from the top and the base of the fractured reservoir interval as a function of offset and azimuth. For modest angles of incidence and small contrasts in acoustic and shear impedance, the only information required for the correction are the angles of SV-SV and SH-SH zero crossings—which tend to occur in a small range of angles, near 20° for SV and 40° for SH for most sedimentary rocks. This correction can be applied to four-component direct shear data at non-zero source-receiver offsets, leading to an extension of the widely applied Alford rotation to non-zero angles of incidence. Such corrections may lead to improved capability of polarization information for analysis of anisotropic properties in the subsurface.

Limitations of shear-wave rotation analyses include the impact of transmission through shallow anisotropic media, which impose polarities on the recorded shear data—masking further polarization analysis. Layer stripping schemes have been implemented have been implemented to current Alford rotation analyses to overcome this effect. Adaption of such layer-stripping to the non-zero offset case is the next logical step in the extension of Alford rotation methods to non-normal angles of incidence.

ACKNOWLEDGEMENTS

We acknowledge the Jackson School of Geosciences, Univ. of Texas-Austin and the industry sponsored EDGER Forum in the Dept. of Geological Sciences, UT-Austin for their support.

REFERENCES

Alford, R. M., (1986) Shear data in the presence of azimuthal anisotropy, Dilley Texas— Expanded Abstracts, 56th Annual International Mtg, Soc. of Exploration Geophysicists, 476-479.

Campbell, T., and Tatham, R. H. (2011) Correction for distortion in polarization of reflected shear- waves in isotropic and anisotropic media, Expanded Abstracts, 81st Annual Intl. Mtg, Soc. of Explor. Geophysicists, 30, 1333-1337

Campbell, T. and Tatham, R. H. (2012) Corrections for polarization distortion in reflected shear Waves and possible extensions to the Alford rotation at non-normal incidence angles and applications—Expanded Abstracts, Vol. 31, 82nd Annual Intl. Mtg, Soc. of Explor. Geophysicists 31, MS E-P1-1.8

Gumble, J. E. (2006) Complete anisotropic analysis of three component seismic data related to the Marine environment and comparison to nine component land seismic data: Ph.D. dissertation, University of Texas at Austin.

Lyons, E. S. (2006) Polarization rotation upon reflection of direct shear waves in purely isotropic media: M.S. thesis, University of Texas at Austin.

Mallick, S., and L. N. Frazer (1987) Practical aspects of reflectivity modeling: Geophysics, 52, 1355–1364.

Spratt, R. S., N. R. Goins, & T. J. Fitch (1993) Pseudo-shear—The analysis of AVO, in M. M. Backus, ed., Offset-dependent reflectivity—Theory & Practice of AVO analysis: SEG

Tatham, R. H. and M. D. McCormack, 1991, Multicomponent Seismology in Petroleum Exploration: SEG, Edited by E. B. Nietzel and D. F. Winterstein.

Thomsen, L. (1986) Weak elastic anisotropy: Geophysics, 51, 1954–1966.